

# Usability assessment of cone beam computed tomography with a full-fan mode bowtie filter compared to that with a half-fan mode bowtie filter

W.K. Choi<sup>1,2</sup>, W. Park<sup>1</sup>, S. Kim<sup>2\*</sup>

<sup>1</sup>Department of Radiation Oncology, Samsung Medical Center, Sungkyunkwan University School of Medicine, Seoul, Korea

<sup>2</sup>Department of Radiological Science, Gachon University, Hambangmoe-ro, Yeonsu-gu, Incheon, Korea

## ABSTRACT

**Background:** In intensity modulated radiation therapy, cone beam computed tomography (CT) has been used to evaluate patients prior to treatment. This study conducted a comparative evaluation of the image reconstruction ability of the clinically used half-fan bowtie filter and the full-fan bowtie filter. **Materials and Methods:** A CT simulation marker was inserted inside a human phantom, and the pelvic region, a large field-of-view region, was scanned by moving the isocenter along the x-axis  $\pm 1-5$  cm with the full-fan mode. Furthermore, image verification was conducted based on the planning CT image and bone to confirm the setup correction value. The obtained value was then compared with that from the clinically used half-fan scan. **Results:** The evaluation of the reconstructed image (from the isocenter to the marker) after setting the median line did not show a significant difference with respect to the image obtained using the half-fan scan. Planning CT images and setup errors were compared in three directions, and the results showed that each mean value was within the margin of error ( $\pm 3$  mm). The 3D vector value was determined to be within 0–2.45 mm, and the comparison of the value obtained from the half-fan scan showed no statistically significant result. **Conclusion:** The application of a phantom study to actual patients in the future will reduce the error caused by movement during the treatment due to the short scan time and will reduce the imaging dose for patients during setup error confirmation and correction.

**Keywords:** CBCT, bowtie filter, imaging dose, Full fan mode, half fan mode.

## ► Technical Note

**\*Corresponding authors:**  
Sungchul Kim, PhD.,  
E-mail: [ksc@gachon.ac.kr](mailto:ksc@gachon.ac.kr)

Revised: October 2019  
Accepted: January 2020

Int. J. Radiat. Res., January 2021;  
19(1): 231-237

DOI: 10.29252/ijrr.19.1.231

## INTRODUCTION

Accurate treatment can be difficult during fractionated radiotherapy due to multiple factors, including changes in patient position, patient weight loss over the course of treatment, and the motion of internal organs. To address these problems, various imaging modalities for confirming the patient setup prior to treatment have been developed. Among these, the utilization of cone beam computed tomography

(CBCT) using an on-board imager (OBI) has increased of late.

CBCT can create volumetric images by reconstructing 360–720 projection data from one rotation using a kilo voltage (kV) radiation source and the kV detector attached to the gantry. It has been developed into a three-dimensional (3D) imaging method for image-guided radiation therapy (IGRT), which produces images of the patient and allows adjustment of the patient position by providing

information on the target location and organ at risk (OAR) <sup>(1-2)</sup>. However, the overall treatment time has increased as the time for obtaining reconstructed images was added to the existing treatment process. Furthermore, CBCT has more artifacts than typical computed tomography (CT), as well as lower imaging quality and lower CT number accuracy. In addition, the patient's radiation exposure doses were increased by the 600–700 X-rays taken within 1 minute. This presents a potential problem as a regular setup correction method in the course of fractionated radiation therapy <sup>(3)</sup>.

The effects of anatomic changes, such as organ deformation, tumor shrinkage, and weight loss, and setup inaccuracy, however, were significantly reduced by 5–8% as fractionated irradiation progressed <sup>(4)</sup>. When this change is clinically significant, the original treatment plan should be modified to deliver the intended dose prior to additional treatment <sup>(5)</sup>. In current clinical practice, CBCT is always conducted up to 20–40 times prior to treatment to identify changes in the factors necessary for treatment during intensity-modulated radiation therapy (IMRT) and to allow for the prompt application of adaptive radiation therapy (ART), as well as the adjustment of existing planning CT images and setup errors by checking the images prior to treatment. Numerous studies on dose calculation based on CBCT images related to ART have already been conducted <sup>(4,6-9)</sup>.

CBCT image acquisition is mostly conducted to correct setup error adjustments. When adjusting, the well-visualized bone in the image, which exhibits less movement and fewer changes in the region of interest (ROI), is set as a reference. In certain situations, adjustment can be done with the target or adjacent OAR.

An aluminum bowtie filter is used for CBCT image acquisition for adjustment purposes. This filter decreases the scattering, beam-hardening, and charge-trapping effects in the detector <sup>(10,11)</sup>. In addition, it compensates for the heel effect by equalizing the detector's current amount <sup>(12)</sup>. The bowtie filter generally reduces the patient's skin dose and improves the quality of the image obtained <sup>(11)</sup>. In radiation therapy, there are two types of bowtie filter by field of view (FOV) size

that can be used for CBCT scans, and both were used in this study. The head and neck region, which has a small FOV, uses a full-fan scan by rotating the gantry 200°; the thorax or pelvic region, on the other hand, which has a large FOV, uses a half-fan scan by rotating the gantry 360°. Although the half-fan scan produces good-quality images for numerous projection data, it has a longer scan time than the full-fan scan, thus increasing the consequent imaging dose <sup>(13)</sup>.

Considerable effort is required to shorten the scan time and decrease the imaging dose for patients. Previous studies investigated the changes in CBCT images by FOV and patient size using CT number values <sup>(14)</sup> and evaluated the exposure dose and image quality for different CBCT scan modes <sup>(15)</sup>. Both these studies used the Catphan 504 phantom (The Phantom Laboratory, Salem, NY, USA) and solid water phantom (Gammex-RMI, Middleton, WI, USA) which are both applicable to CBCT quality assurance (QA). Their application to patients, however, is limited due to the small size of the QA phantom and lack of anatomical information.

Therefore, in this study, a human phantom was used with two methods (half-fan scan and full-fan scan) for imaging of the large-FOV pelvic region, for which the half-fan scan is typically used. The scan ranges and image distortion were evaluated by measuring the distances between points in the reconstructed CBCT image. Values from the full-fan scan were compared to those obtained from the half-fan scan and error correction values of the planning CT of the two scan types were then compared.

## **MATERIALS AND METHODS**

### ***Image acquisition***

In this study, the pelvic region of a human phantom (RANDO®, Alderson Research Laboratories Inc., Stanford, CT, USA), which has a large FOV, was used. To mark the location of the isocenter during the planning CT scan, the most commonly used CT simulation marker was inserted inside the human phantom. The median line, mid-depth of the pelvis, was set as the

virtual isocenter, and a total of 10 markers, including the isocenter, were inserted at certain distances in a radial shape (figure 1).

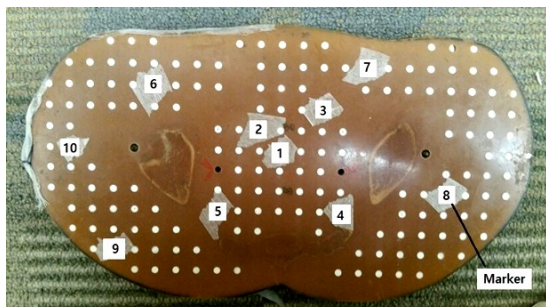


Figure 1. RANDO® phantom slice with CT simulation marker.

Planning CT images were obtained in the helical mode using a CT scanner (Discovery RT590, GE, USA), whose use in this study was allowed by the manufacturer on the condition that it would be clinically used and following the protocol recommended by the company. After completion of the scan, the images were sent to Pinnacle (Pinnacle<sup>3</sup>, Philips, USA), the program used for radiation therapy planning (RTP) in the authors' institution. The treatment plan was set as radiating a single fixed beam with the isocenter close to the center of the planning target volume. The virtual plan was applied and obtained data were sent to the treatment room.

The Novalis Tx system (Varian Medical Systems, Palo Alto, CA, USA), a linear accelerator used for IMRT, was used to acquire CBCT images in this study. Among the six modes of treatment-room CBCT imaging acquisition (low-dose head, standard-dose head, high-quality head, pelvic spotlight, pelvis, and low-dose thorax), each image in this study was acquired using the half-fan pelvis mode (655 projection images acquired from 360° gantry rotation), which is used for IMRT of the pelvis region in the authors' institution, and full-fan standard-dose head mode (images acquired from 200° gantry rotation) (table 1).

Table 1. Reference data for CBCT (OBI 1.4).

Bowtie filter	Mode name	Acquisition angle (°)	Technique	Dose (cGy)
Full	Standard-dose head	200	100 kV, 20 mA, 20 ms	0.4
Half	Pelvis	360	125 kV, 80 mA, 13 ms	1.8

Regarding the parameters of the CBCT scan, a 2.5-mm slice thickness and 512×512 resolution method were used, the same as with planning CT images. After the acquisition of CBCT images, they were superimposed on the planning CT images, and 3D/3D matching was conducted based on the outlines of the anatomical structures.

### Image quality analysis

In full-fan scan application, a total of 10 CT simulation markers, including the isocenter (pelvis median line, mid-depth), were inserted inside the human phantom to compare the extent of image distortion and degradation by measuring the scannable range from the measurement distances between isocenter points. The setup was completed based on the isocenter, and scan was conducted by alternating half-fan scan and full-fan scan based on the isocenter. The images were reconstructed, and the distances from each isocenter to the marker were measured as vector values (figure 2).

To identify artifacts due to movement and image range for possible reconstruction, nine distances were measured 11 times after artificially moving the isocenter ±1–5 cm in the latero-medial direction. To improve reliability, a total of 76 measurements were performed using the test-retest method over 3 months at 7-day intervals without geometrical correction of the equipment; the errors were then compared.

### Comparison of the half- and full-fan-scan image verification results

After the superposition of the planning CT images and CBCT images, parallel translation errors towards the x-axis (latero-medial), y-axis (cranio-caudal), and z-axis (antero-posterior) were obtained. Although the couch rotation (yaw) errors are corrected in actual treatment, they were excluded in this comparison study to determine the size of the displacement vector (3D vector) provided by the orthogonal coordinate system.

Image verification was conducted through computerized automatic image verification based on bony anatomy within the ROI after

setting the ROI for 3D matching on the planning CT images (figure 3). If the error after image verification was large, the setup process was repeated. When shift values within the margin of error (margin of error for the pelvis: within  $\pm 3$  mm towards the x-, y-, and z-axis) were found, the information was delivered to the linear accelerator and the couch automatically moved to correct the positioning error. Based on this principle, the study was conducted in the same way as actual treatment.

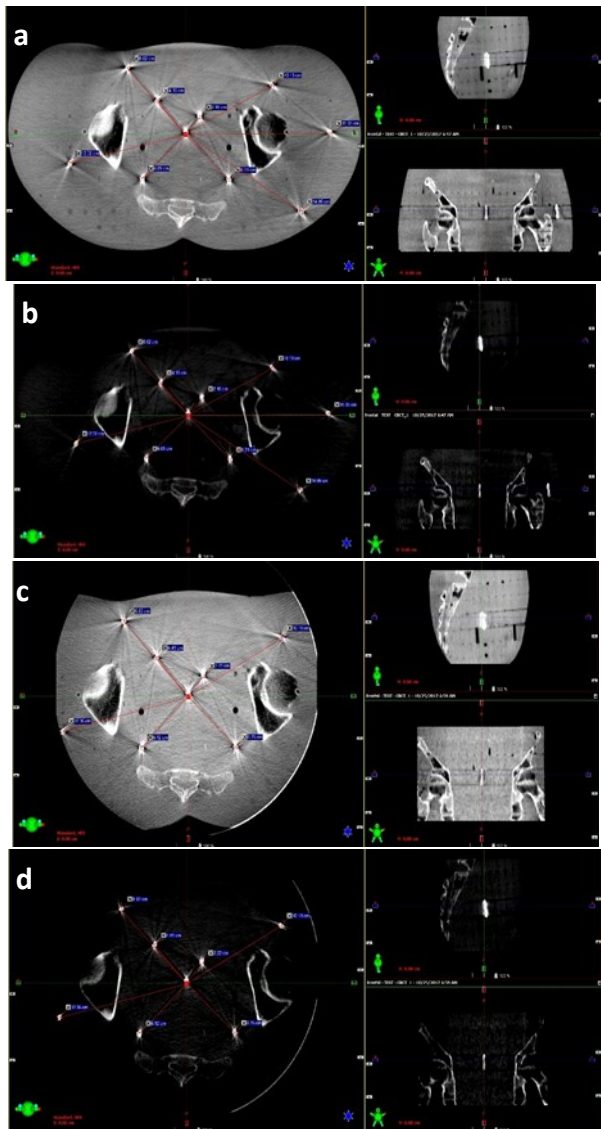


**Figure 2.** Half-fan/full-fan scan image and distance analysis. **a)** Half-fan scan image. **b)** Half-fan scan distance analysis. **c)** Full-fan scan image. **d)** Full-fan scan distance analysis.

The corrected error values were calculated through the 3D/3D matching of the obtained

CBCT and planning CT images to compare the half- and full-fan scan modes. In addition, the 3D vector value, the index of the displacement results from the reference point, was calculated using equation 1 (16).

$$3D \text{ vector} = \sqrt{x^2 + y^2 + z^2} \quad (1)$$

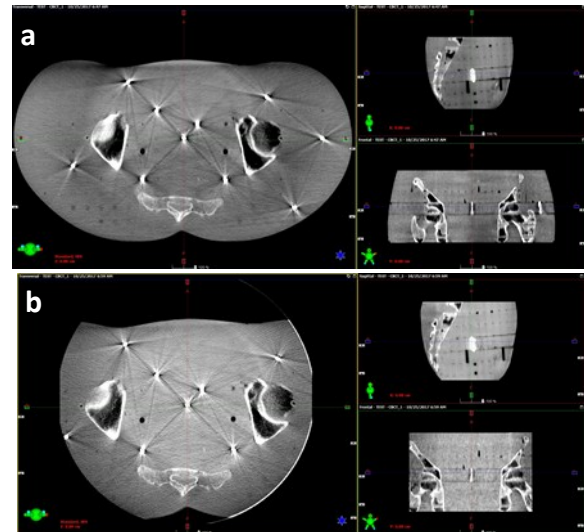


**Figure 3.** Half-fan/full-fan scan image verification analysis. **a)** Half-fan scan verification analysis. **b)** Half-fan/full-fan scan image verification analysis

Similar to the imaging analysis, the isocenter was artificially moved by  $\pm 1-5$  cm in the latero-medial direction and was scanned with two modes 11 times. Changes in the error correction value were then identified. To obtain the necessary sample size for statistical analysis and investigate the changes that occur over time, measurements were performed a total of 12 times over 3 months and 264 data were analyzed.

### Statistical analysis

As there are several measured samples in the study the statistical significance was tested by multiple comparison (19). A two-way ANOVA F-test for repeated measurements was used for this purpose and to see if the difference between half-fan and full-fan between the different methods is statistically significant. P-value was calculated using analysis of variance (ANOVA), and the significance level was set at 0.05. Statistical analysis was conducted using SPSS (ver. 22.0) software (IBM, New York, USA).

## RESULTS

### Image quality analysis

The distance values were measured 76 times and the errors were compared. The maximum error was 2.1 mm, the minimum error was 0 mm, and the mean error was  $0.19 \pm 0.27$  mm. There was no statistically significant difference between the reconstructed images from half- and full-fan scans (table 2).

**Table 2.** Comparison of the distance measurements between the isocenter and CT simulation marker.

Setup (n=76)	Max. deviation	Min. deviation	Mean deviation $\pm$ SD	P-value
Half-fan scan	2.1 mm	0 mm	$0.19 \pm 0.27$ mm	0.98
Full-fan scan				

In addition, although only 0.5 cm thick, a band of approximately 15 cm in diameter was found to have been formed based on the central axis of the OBI due to a beam hardening (cupping) artifact during the image evaluation process for full-fan scan images. Compared to the half-fan scan images, it did not affect the image evaluation (figure 2).

### Comparison of the half- and full-fan-scan image verification results

The 3D reconstructed images were superimposed on the planning CT images and error correction values were calculated using the 3D/3D auto matching method. Similar to the distance measurement study, the isocenter was moved and 11 error correction values were measured 12 times over 3 months, yielding 132 measurements. When the half-fan scan was used, the mean values were  $0.69 \pm 0.55$  mm in the x-axis,  $0.85 \pm 0.49$  mm in the y-axis, and  $0.98 \pm 0.51$  mm in the z-axis. When the full-fan scan was used, on the other hand, the mean values were  $0.82 \pm 0.55$  mm in the x-axis,  $0.86 \pm 0.54$  mm in the y-axis, and  $0.92 \pm 0.59$  mm in the z-axis (table 3). The mean 3D vector values, which represent the 3D parallel displacement in 3D spaces, were  $1.63 \pm 0.54$  mm for the half-fan scan and  $1.72 \pm 0.46$  mm for the full-fan scan. As a result of one-way ANOVA in each direction, there was no difference between

half-fan and full-fan scans in all directions (table 3). The results of two-way batch analysis of repeated differences between the three directions and Bowtie-filter showed no difference between half-fan and full-fan ( $p > 0.05$ ).

**Table 3.** Comparison of the localization accuracy of the half- and full-fan scan modes.

Displacement direction		Half-fan scan mode Mean $\pm$ SD (n=132)	Full-fan scan mode Mean $\pm$ SD (n=132)	P-value
Translation (mm)	LR (x-axis)	$0.69 \pm 0.55$	$0.82 \pm 0.55$	0.06
	SI (y-axis)	$0.85 \pm 0.49$	$0.86 \pm 0.54$	0.90
	AP (z-axis)	$0.98 \pm 0.51$	$0.92 \pm 0.59$	0.37
	3D vector	$1.63 \pm 0.54$	$1.72 \pm 0.46$	0.14

\* LR: left-right; SI: superior-inferior; AP: anterior-posterior

## DISCUSSION

Many studies have been conducted to minimize patients' exposure to radiation during radiation therapy. Special treatment modalities, such as IMRT and IGRT, involve treating a patient after the confirmation and correction of their setup.

The purpose of this study was to reduce the scanning time and minimize patients' radiation exposure during daily CBCT scanning to confirm the patient's setup and verify the clinical applicability of the full-fan bowtie filter compared to the half-fan bowtie filter, which is commonly used clinically for large FOV regions.

Some researchers have conducted studies on scanning time and imaging dose exposure when utilizing the bowtie filter. When the CT dose index was calculated using the ion chamber and Monte Carlo simulation, although only slight differences from the reference book values (0.6 cGy for the standard-dose head, 2.54 cGy for the pelvis) were found, an approximately fourfold difference between the half-fan and full-fan scan was shown by the utilization of the bowtie filter (17). Another study compared the effect of the system version on CBCT imaging radiation dose.

The effective dose for the full-fan scan of the head region was 0.18 mSv and that for the half-fan scan of the pelvic region was 0.51 mSv<sup>(18)</sup>. The scan times showed an approximately 20-s difference between the half-fan (1 minute) and full-fan scan (40 seconds). From the evaluation of the scannable region and image distortion extent using a human phantom, it was found that the patient's exposure dose can be reduced by reducing the test time when the fullfan mode is applied.

Based on the obtained results, when a full-fan scan was used, the scan region did not move away from the central axis of rotation, and there was no image distortion or deformation from the movement of the isocenter. When auto-correction was conducted based on the original image within the ROI, however, the auto-correction 3D vector value of the full-fan scan was 0–2.45 mm less than that of the half-fan and was within the margin of error, which is within 3 mm of the mean value. Another study that evaluated the error correction values also determined that they were within the 3 mm mean value, with autocorrection values ranging 1.1–4.9 mm in the pelvic region. Myriad data have already been reported using not only CBCT, but also an electronic portal imaging device (EPID), film, and L-gram<sup>(19)</sup>.

It was found, however, that the range of reconstructed images was small due to the limited FOV and that severe artifacts had developed. The artifacts caused by obtaining projecting images with one rotation of a large-FOV region are due to the strongly scattered X-rays and can cause CT number inaccuracy, decreased contrast, and space non-uniformity. As of yet, there is no clear solution<sup>(20)</sup>. This notwithstanding, it did not affect image evaluation and movement correction value studies. Furthermore, this study did not consider the effects of the target size. The study had a limitation in that if it goes beyond the full-fan scan region or if there is an artifact affecting anatomical information that is used as a reference for image verification depending on the target size and location, the clinical applicability of the full-fan bowtie filter compared to the half-fan bowtie filter may not

be applicable.

## CONCLUSION

Based on the results of this study, the application of full-fan scan based on the target size and location must be considered when treating a large FOV region in clinical practice, rather than unconditional application of the half-fan scan and is considered capable of reducing the imaging dose to be administered to the patients when confirming and correcting setup error and of decreasing error occurrence caused by movement during treatment, due to the shorter scan time.

*Conflicts of interest: Declared none.*

## REFERENCES

1. Jaffray DA and Siewerdsen JH (2000) Cone-beam computed tomography with a flat-panel imager: initial performance characterization. *Med Phys* 2000, **27**(6): 1311-23.
2. Hansen EK, Bucci MK, Quivey JM, Weinberg V, Xia P (2006) Repeat CT imaging and replanning during the course of IMRT for head-and-neck cancer. *Int J Radiat Oncol Biol Phys*, **64**(2): 355-362.
3. Islam MK, Mohammad K Islam 1, Purdie TG, Norrlinger BD, Alasti H, Moseley DJ, Sharpe MB, Siewerdsen JH, Jaffray DA (2006) Patient dose from kilovoltage cone beam computed tomography imaging in radiation therapy. *Med Phys*, **33**(6): 1573-1582.
4. Lee L, Le QT, Xing L (2008) Retrospective IMRT dose reconstruction based on cone-beam CT and MLC log-file. *Int J Radiat Oncol Biol Phys*, **70**(2): 634-44.
5. Karellas A, Lo JY, Orton CG (2008) Point/counterpoint. Cone beam X-ray CT will be superior to digital X-ray tomography in imaging the breast and delineating cancer. *Med Phys*, **35**(2): 409-411.
6. Ding GX, Duggan DM, Coffey CW, Deeley M, Hallahan DE, Cmelak A, Malcolm A (2007) A study on adaptive IMRT treatment planning using kV cone-beam CT. *Radiation Oncol*, **85**(1): 116-125.
7. Nijkamp J, Pos FJ, Nuver TT, de Jong R, Remeijer P, Sonke JJ, Lebesque JV (2008) Adaptive radiotherapy for prostate cancer using kilovoltage cone-beam computed tomography: first clinical results. *Int J Radiat Oncol Biol Phys*, **70**(1): 75-82.

8. Yoo S and Yin FF (2006) Dosimetric feasibility of cone-beam CT-based treatment planning compared to CT-based treatment planning. *Int J Radiat Oncol Biol Phys*, **66**(5): 1553-1561.
9. Richter A, Hu Q, Steglich D, Baier K, Wilbert J, Guckenberger M, Flentje M (2008) Investigation of the usability of conebeam CT data sets for dose calculation. *Radiat Oncol*, **3**: 42.
10. Mail N, Moseley D, Jaffray D (2009) The influence of bowtie filtration on cone-beam CT image quality. *Med Phys*, **36**(1): 22-32.
11. Siewerdsen JH and Jaffray DA (2001) Cone-beam computed tomography with a flat-panel imager: magnitude and effects of x-ray scatter. *Med Phys*, **28**(2): 220-231.
12. Glover GH (1982) Compton scatter effects in CT reconstructions. *Med Phys*, **9**(6): 860-867.
13. Kumar AS, Singh IRR, Sharma SD, John S, Ravindran BP (2016) Radiation dose measurements during kilovoltage-cone beam computed tomography imaging in radiotherapy. *J Cancer Res Ther*, **12**(2): 858-863.
14. Seet, KY, Barghi A, Yartsev S, Van Dyk J (2009) The effects of field-of-view and patient size on CT numbers from cone-beam computed tomography. *Phys Med Biol*, **54**(20): 6251-6262.
15. Kim S and P Alaei (2016) Implementation of full/half bowtie filter models in a commercial treatment planning system for kilovoltage cone-beam CT dose estimations. *J Appl Clin Med Phys*, **17**(2): 153-164.
16. Lin CG, Xu S, Yao W, Wu Y, Fang J, Wu V *et al.* (2017) Comparison of set up accuracy among three common immobilisation systems for intensity modulated radiotherapy of nasopharyngeal carcinoma patients. *J Med Radiat Sci*, **64**(2): 106-113.
17. Kim S, Yoo S, Yin F, Samei E, Yoshizumi T *et al.* (2010) Kilovoltage cone-beam CT: comparative dose and image quality evaluations in partial and full-angle scan protocols. *Med Phys*, **37**(7):3648-3659.
18. Cheng HC, Wu VW, Liu ES, Kwong DL *et al.* (2011) Evaluation of radiation dose and image quality for the Varian cone beam computed tomography system. *Int J Radiat Oncol Biolo Phys*, **80**(1): 291-300.
19. Hurkmans C, Remeijer P, Lebesque J, Mijnheer B *et al.* (2001) Set-up verification using portal imaging; review of current clinical practice. *Radiotherapy and oncology*, **58**(2): 105-120.
20. Niu T and Zhu L (2011) Scatter correction for full-fan volumetric CT using a stationary beam blocker in a single full scan. *Medical Physics*, **38**(11): 6027-6038.

